


Theoretical prediction of a non-Hermitian skin effect in ultracold-atom systems

Sibo Guo^{1,2,*}, Chenxiao Dong^{1,2,*}, Fuchun Zhang^{3,†}, Jiangping Hu^{1,2,3,‡} and Zhesen Yang^{3,§}

¹Beijing National Laboratory for Condensed Matter Physics and Institute of Physics, Chinese Academy of Sciences, Beijing 100190, China

²School of Physical Sciences, University of Chinese Academy of Sciences, Beijing 100049, China

³Kavli Institute for Theoretical Sciences, University of Chinese Academy of Sciences, Beijing 100190, China

 (Received 15 November 2021; revised 29 June 2022; accepted 5 December 2022; published 20 December 2022)

We study the non-Hermitian skin effect in dissipative ultracold fermions with spin-orbit coupling, which has been implemented in a recent experiment (Z. Ren *et al.*, *Nat. Phys.* **18**, 385 (2022)). In this work we prove that the non-Hermitian skin effect in such a continuous system is robust to the variation of external parameters and trapping potentials. We further reveal a dynamic sticky effect in our system, which has a common physical origin with the non-Hermitian skin effect. Our work paves the way for studying novel physical responses of the non-Hermitian skin effect in quantum systems.

DOI: [10.1103/PhysRevA.106.L061302](https://doi.org/10.1103/PhysRevA.106.L061302)

I. INTRODUCTION

The ultracold-atom system has provided an ideal platform for studying both single-particle physics and many-body physics due to its super purity, high controllability, and intrinsic quantum nature [1–5]. Some examples include the study of topological band theory [6–24] and strongly correlated physics [2,25–28]. When the system is not closed, particles can escape from the system to the environment [29–46] and its single-particle physics can no longer be described by a Hermitian Hamiltonian, but by an effective non-Hermitian Hamiltonian [45,47,48]. For example, recently, Ref. [36] first implemented a one-dimensional spin-orbit-coupled system with highly controllable spin-dependent particle loss, which establishes a new platform to study non-Hermitian physics.

The non-Hermitian skin effect (NHSE), which refers to an anomalous localization phenomenon in an open boundary system [49], has been widely studied recently [49–77]. For a system with the NHSE, the number of boundary localized eigenstates is proportional to the volume of the system. From a theoretical point of view, an important implication of the NHSE is the nonperturbative breakdown of Bloch's theorem [78], which introduces new opportunities and challenges to quantum theories established within Bloch's theorem. From an experimental point of view, although the NHSE has been experimentally observed in several classical systems [68–71,79–84], its implementation in quantum systems is still absent. Therefore, the realization and detection of the NHSE in quantum systems, e.g., ultracold-atom systems, have become the next step for the non-Hermitian community and may open a new route for further theoretical research.

In this paper we predict that the one-dimensional dissipative spin-orbit-coupled ultracold fermions implemented in Ref. [36] have a robust NHSE. In contrast to previous studies of the lattice model, the NHSE discussed in this paper appears in a continuous model due to the absence of an externally applied optical lattice. We also generalize the non-Bloch band theory [49,53,56] to the continuous case, which is referred to as generalized wave vector (GWV) theory. In addition, we propose that the NHSE in our model can induce a so-called momentum-dependent dynamic sticky effect (DSE), that is, when a small (large) momentum wave packet hits the skin-localized boundary, it will be bounded (reflected) by the corresponding boundary.

II. NHSE IN ULTRACOLD ATOMS

The model implemented in Ref. [36], which is illustrated in Fig. 1(a), can be described by the stationary Schrödinger equation

$$[H(\hat{k}) + V(x)]\psi_E(x) = E\psi_E(x), \quad (1)$$

where $\hat{k} = \hat{p}/\hbar = -i\partial_x$ is the wave-vector operator, $V(x)$ is the effective trapping potential, and $H(\hat{k})$ is the free-particle Hamiltonian whose form is

$$H(\hat{k}) = \begin{pmatrix} \epsilon_-(\hat{k}) + \delta/2 - i\Gamma_{\uparrow}/2 & \Omega_R/2 \\ \Omega_R/2 & \epsilon_+(\hat{k}) - \delta/2 - i\Gamma_{\downarrow}/2 \end{pmatrix}. \quad (2)$$

Here $\epsilon_{\pm}(\hat{k}) = (\hbar\hat{k} \pm \hbar q_r)^2/2m$, m is the mass of the atom, $\pm\hbar q_r$ is half of the momentum transferred through the two-photon Raman coupling process with Raman coupling strength Ω_R and two-photon detuning δ [85], and $\Gamma_{\uparrow(\downarrow)}$ is proportional to the spin-dependent loss of the atom.¹

*These authors contributed equally to this work.

†Corresponding author: fuchun@ucas.ac.cn

‡Corresponding author: jphu@iphy.ac.cn

§Corresponding author: yangzs@ucas.ac.cn

¹Here we define the recoil momentum $\hbar q_r$ and recoil energy $E_r = \hbar^2 q_r^2/2m$ as the units of momentum and energy, respectively. The corresponding derivation of the dimensionless Hamiltonian can be found in the Supplemental Material [86].

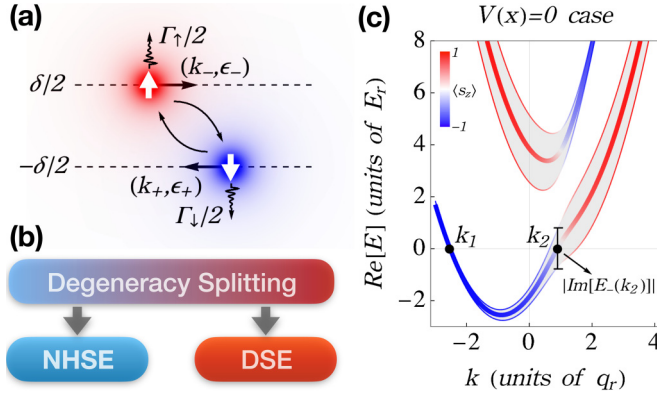


FIG. 1. (a) Physical system we studied where $k_{\pm} = k \pm q_r$ and $\epsilon_{\pm} = \hbar^2 k_{\pm}^2 / 2m$. (b) Both the NHSE and the DSE originate from the (free-particle spectral) degeneracy splitting. (c) Presence of degeneracy splitting in our model. One can find that although the real part of the energy between states k_1 and k_2 is the same, the imaginary part of the energy is different. The parameters are $(\delta, \Omega_R, \Gamma_{\uparrow}, \Gamma_{\downarrow}) = (4, \frac{9}{2}, 6, \frac{6}{13})E_r$, where $E_r = \hbar^2 q_r^2 / 2m$.

When the effective trapping potential $V(x)$ is ignored, the atoms can be considered free. By diagonalizing Eq. (2) we can obtain the corresponding eigenvalues

$$E_{\pm}(k) = E_0(k) \pm \sqrt{\left(-\frac{\hbar^2 q_r}{m} k + \frac{\delta}{2} - i\frac{\Gamma_z}{2}\right)^2 + \frac{\Omega_R^2}{4}}, \quad (3)$$

where $k \in \mathbb{R}$, $E_0(k) = \hbar^2(k^2 + q_r^2)/2m - i\Gamma_0/2$, and $\Gamma_0(z) = (\Gamma_{\uparrow} \pm \Gamma_{\downarrow})/2$. As shown in Fig. 1(b), an important feature of Eq. (3) is the presence of (free-particle spectral) degeneracy splitting,² which causes the NHSE and DSE. The reason is that due to the existence of degeneracy splitting, the number of plane waves is not enough to form the eigenstate (and participate in the boundary reflection process), which indicates the emergence of the NHSE (and DSE). This degeneracy splitting can be observed in Figs. 1(c) and 2(a). In Fig. 1(c), $\text{Re} E_{\pm}(k)$ is plotted with thick solid lines and $\text{Re} E_{\pm}(k) + |\text{Im} E_{\pm}(k)|/2$ and $\text{Re} E_{\pm}(k) - |\text{Im} E_{\pm}(k)|/2$ are plotted with thin solid lines. Therefore, the vertical distance around $\text{Re} E_{\pm}(k)$ represents $|\text{Im} E_{\pm}(k)|$. One can find that although $\text{Re} E_{-}(k_1) = \text{Re} E_{-}(k_2) = 0$, their imaginary parts are different. Other parameters in the calculation are listed in the caption of the corresponding figures, and the color of the curves represents the mean value of the z -component spin, i.e., $\langle s_z \rangle$.³ Figure 2(a) further shows that the above-discussed degeneracy splitting still holds in almost the whole spectrum in the plotted region. Here we note that the solid lines and arrows in Fig. 2(a) indicate the spectral flow in the complex energy plane when k runs from $-\infty$ to $+\infty$.

²The degeneracy splitting proposed here is for the whole spectrum. There may be a few intersection points in the spectrum at which no splitting occurs, so the state formed by these corresponding eigenstates may not be localized at the boundary, which is an extended state.

³More precisely, $\langle s_z \rangle = \langle u_{\pm}^R(k) | s_z | u_{\pm}^R(k) \rangle$, where $|u_{\pm}^R(k)\rangle$ is the right eigenstate [87] of Eq. (2) with eigenvalue $E_{\pm}(k)$.

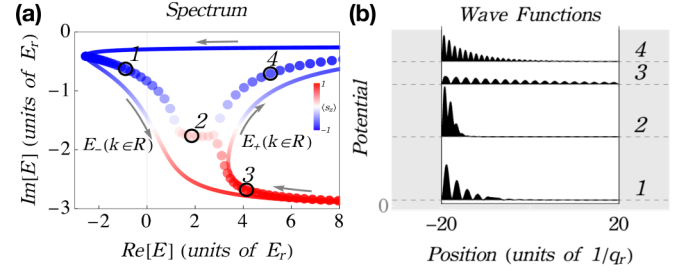


FIG. 2. (a) Energy spectrum of Eq. (1), where solid lines represent the spectrum under $V(x) = 0$ and the dots represent the spectrum under Eq. (4) with $L = 40/q_r$. (b) Several eigenfunctions whose eigenvalues are labeled in (a). Both the spectral difference and the exponential localization of the eigenfunctions are the signatures of the NHSE. The parameters are the same as in Fig. 1.

When the effective trapping potential $V(x)$ is taken into account, the NHSE appears. In order to simplify the discussion, a box potential is assumed, i.e.,

$$V(x) = \begin{cases} 0 & \text{for } -L/2 < x < L/2 \\ \infty & \text{otherwise.} \end{cases} \quad (4)$$

As shown in Fig. 2(a), the dots represent the numerical solutions in the drawing interval with $L = 40/q_r$ for Eq. (4). One can find that the eigenvalues in the box potential are distinct from the free-particle spectrum $E_{\pm}(k \in \mathbb{R})$ in the complex energy plane. This is the spectral signature for the emergence of the NHSE [54,55]. Figure 2(b) further shows several typical numerical wave functions of the system, whose eigenvalues are labeled in Fig. 2(a).⁴ One can find that they are all exponentially localized at the left boundary and have different localization lengths. The appearance of the exponentially localized eigenstates for the quasicontinuous spectrum is the wave-function signature for the emergence of the NHSE [49,53].

III. ASYMPTOTIC SOLUTIONS

For large L , the asymptotic solution of Eq. (1) for the box potential (4) can be obtained analytically, which contains two boundary-condition-allowed complex wave-vector curves k_+ and k_- , respectively. The corresponding asymptotic eigenspectra of E_+ and E_- can be obtained from $E_+(k_+)$ and $E_-(k_-)$, respectively [86]. Here we note that our method can be regarded as a continuous version of the auxiliary generalized Brillouin zone theory [56]. As shown in Figs. 3(a) and 3(b), the thick solid colored lines represent the asymptotic curves of complex wave vectors k_+ and k_- , which we call GWVs, and the thin solid gray lines represent the auxiliary generalized wave vectors, which determine the analytical behaviors of k_{\pm} and can be calculated exactly [86]. From Figs. 3(a) and 3(b) one can find that $\text{Im} k_{\pm}$, which is related to the localization behaviors, gradually approaches zero as

⁴Here we note that the wave functions we plotted are $|\psi_{E_i, \uparrow}(x)|^2 + |\psi_{E_i, \downarrow}(x)|^2$, where $\psi_{E_i, \uparrow(\downarrow)}(x)$ is the spin-up (-down) component of the eigenfunction whose eigenvalue is E_i .

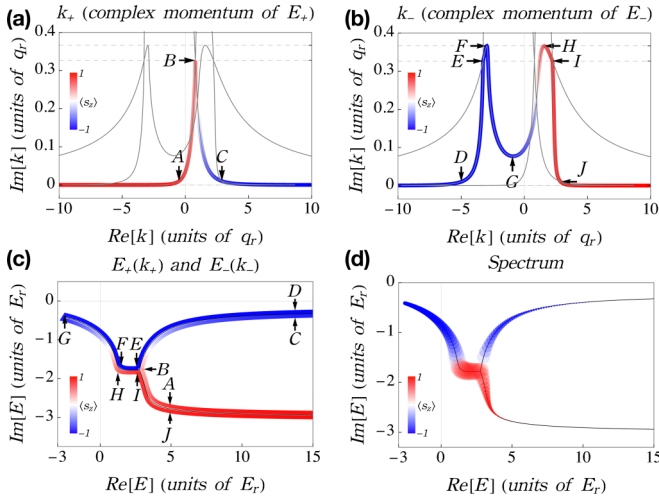


FIG. 3. Asymptotic solutions under the parameters shown in Fig. 1. In (a) and (b) the generalized wave vectors and auxiliary generalized wave vectors are shown with thick colored lines and thin gray lines, respectively. Here the dashed lines represent the largest and smallest values of the imaginary part of k , respectively, which will be used to characterize the strength of the NHSE [86]. (c) Asymptotic spectrum, namely, E_+ (E_-) maps the curve $A-B-C$ ($D-E-F-G-H-I-J$) (represent the energy flow for $E_+(k_+)$ [$E_-(k_-)$]) in (a) [(b)] to the curve $A-B-C$ ($D-E-F-G-H-I-J$) in (c). (d) Comparison between the asymptotic (black line) and numerical (colored dots) solutions. Here the radius of the dots in (d) is proportional to the inverse of the localization length.

$|\text{Re } k_{\pm}|$ increases.⁵ As a result, the corresponding asymptotic eigenstate becomes extended. In contrast, the eigenstates for small $|\text{Re } k_{\pm}|$ are localized skin modes. Figure 3(c) shows the asymptotic spectrum determined by k_{\pm} , where the point pairs (F, H) , (E, B, I) , (A, J) , and (C, D) represent four different common points in the complex energy plane. It should be noted that $E_+(k_+)$ and $E_-(k_-)$ cover different regions in the complex plane, respectively [86]. As shown in Fig. 3(d), by comparing $E_{\pm}(k_{\pm})$ with numerical solutions represented by the dots in Fig. 3(d) one can find that they match well.

IV. ROBUSTNESS OF THE NHSE

The stability of the NHSE is related to the absence of the inversion symmetry \mathcal{P} and anomalous time-reversal symmetry $\bar{\mathcal{T}}$ [65,88] of $H(k)$, whose definitions are

$$\mathcal{P}^{-1}H(k)\mathcal{P} = H(-k), \quad \bar{\mathcal{T}}^{-1}H(k)\bar{\mathcal{T}} = H(-k), \quad (5)$$

where k is a complex number, \mathcal{P} is a unitary operator, and $\bar{\mathcal{T}} = U_{\bar{\mathcal{T}}}\mathcal{K}^t$ is an antiunitary operator with \mathcal{K}^t the transpose operator [88,89]. It can be checked that once $\Gamma_{\uparrow} \neq \Gamma_{\downarrow}$, the two symmetries above must be broken, which ensures the existence of the NHSE. Further numerical verifications are shown in the Supplemental Material [86].

⁵For example, here the points A and C represents the position at which $\text{Im}(k_+) = 1/100$ and the points D and J that at which $\text{Im}(k_-) = 1/100$.

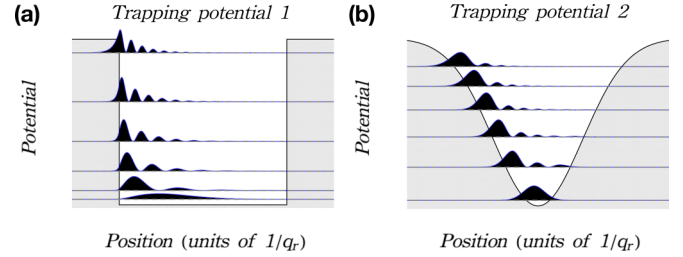


FIG. 4. Spatial distribution of several eigenfunctions in (a) a finite deep square well and (b) a Gaussian well [86], where the presence of the skin modes localized on the left can be clearly seen. The parameters are the same as those in Fig. 1.

The NHSE is also robust against trapping potentials. In Figs. 4(a) and 4(b) we have plotted several eigenstates localized on the left-hand side of the boundary under different trapping potentials, which numerically indicates the robustness of the NHSE [86]. This robustness is quite important, since if the NHSE can be destroyed by these potentials, then the NHSE will be fragile and can hardly be observed in experiments.

We believe that the above robustness of the NHSE to external potentials is a consequence of the non-Hermitian bulk-boundary correspondence. Here the bulk refers to the degeneracy splitting of the free-particle spectrum and the boundary refers to the NHSE under generic slowly varying trapping potentials $V(x)$. The reason is that in the slowly varying trapping region $V(x)$ can be approximated by a constant. As a result, the corresponding solution in this region will not all be composed of plane waves due to the presence of degeneracy splitting.

V. DYNAMIC STICKY EFFECT

Now we reveal a new effect related to the NHSE, that is, the DSE. In general, this effect can be present in any non-Hermitian systems with the NHSE, not restricted to ultracold atoms. Figures 5(a) and 5(b) and Figs. 5(c) and 5(d) show the dynamics of the system without and with the NHSE, respectively. Here the initial state is $\psi_{\uparrow}(x, t=0) = 0$ and $\psi_{\downarrow}(x, t=0) = A \exp[-(x-x_0)^2/20 + ik_0x]$, where A is the normalization factor, the center position $x_0 = 40/q_r$, and the average momentum $k_0 = -3q_r$ in Figs. 5(a) and 5(c) and $k_0 = -5q_r$ in Figs. 5(b) and 5(d). In order to characterize the dynamical evolution of wave packets, we normalized the wave function at each time and plot $|\psi(x, t)| = \sqrt{|\psi_{\uparrow}(x, t)|^2 + |\psi_{\downarrow}(x, t)|^2}$ in Figs. 5(a ii)–5(d ii). An important feature for the dynamics with the NHSE is that the wave packets will be bounded (reflected) at a small (large) momentum k_0 by the left boundary as shown in Fig. 5(c ii) [Fig. 5(d ii)]. This anomalous dynamical behavior is referred to as the momentum-dependent DSE in this paper.

The reason why the DSE appears and is momentum dependent can be well explained by the fact that the DSE has a similar physical origin to the NHSE, that is, the degeneracy splitting as shown in Fig. 1(b). Now we explain it. We first focus on the incident waves. As shown in Figs. 5(a i)–5(d i), the (mean) momentum of the incident wave is k_1

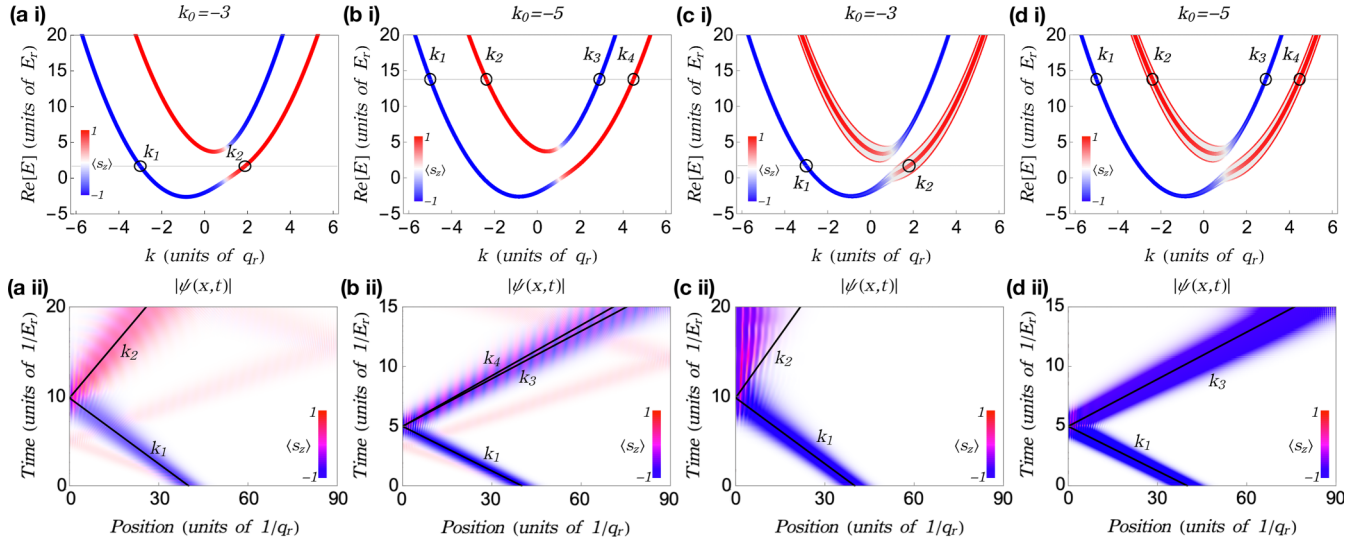


FIG. 5. Dynamical behavior of the system (a) and (b) without NHSE, i.e., $(\delta, \Omega_R, \Gamma_\uparrow, \Gamma_\downarrow) = (4, \frac{9}{2}, 0, 0)E_r$, and (c) and (d) with NHSE, i.e., $(\delta, \Omega_R, \Gamma_\uparrow, \Gamma_\downarrow) = (4, \frac{9}{2}, 6, \frac{6}{13})E_r$. (a i)–(d i) Free-particle dispersion relation $\text{Re} E_\pm(k \in \mathbb{R})$, in which the shadow region represents $|\text{Im} E_\pm(k \in \mathbb{R})|$. (a ii)–(d ii) Scattering behavior of the Gaussian wave packet with a different momentum, in which the solid lines represent the trajectories calculated from the group velocity. The anomalous reflection behavior in (c ii) can be understood from the presence of degeneracy splitting in (c i).

and we can define the corresponding group velocity as $v_1 = \text{Re}[dE_-(k)/dk|_{k=k_1}]$ [86]. The solid lines labeled by k_1 in Figs. 5(a ii)–5(d ii) represent the dynamics determined by v_1 , i.e., $x(t) = x_0 + v_1 t$. One can find that the dynamics of the incident waves can be well described by the group-velocity calculations. Next we focus on the reflection waves. For the case in Fig. 5(a), there is only one reflection channel, i.e., k_2 , which satisfies the equal energy condition, i.e., $E_-(k_1) = E_-(k_2)$. Therefore, the reflection wave can be well described by the group velocity of k_2 , which is demonstrated in Fig. 5(a ii). For the case in Fig. 5(b), since there are two reflection channels, i.e., $E_-(k_1) = E_-(k_3) = E_-(k_4)$, the corresponding reflection wave shows an interference feature and also the corresponding dynamics can be well described by the group-velocity calculations, namely, k_3 and k_4 in Fig. 5(b ii). However, for one case with the NHSE, i.e., Fig. 5(c), the presence of degeneracy splitting implies that there is no plane wave that satisfies the equation energy condition. As a result, the reflection becomes anomalous and the DSE appears.⁶⁷ As a comparison, for another case with the NHSE, the degeneracy splitting between k_1 and k_3 is weak, which implies that the reflection wave can be well described by the group velocity of k_3 . The result in Fig. 5(d ii) demonstrates this point. Here

we note that, due to the degeneracy splitting between k_1 and k_4 , k_4 does not contribute to the reflection wave, which can be observed in Fig. 5(d ii) with the absence of interference for the reflection wave.

VI. DISCUSSION AND CONCLUSION

The degeneracy splitting proposed in this work can be regarded as a band criterion for the emergence of the NHSE. Before our work, a spectral criterion was established based on the spectral winding number of the Bloch Hamiltonian [54,55]. Although this criterion is straightforward in some theoretical calculations, it cannot be applied to the experiments because there is no method to measure the complex energy spectrum directly.⁸ In contrast, our band criterion, i.e., the degeneracy splitting, can be measured directly, for example, by angle-resolved photoemission spectroscopy. Therefore, this criterion will be helpful in experiments.

The GWV theory proposed in this work also provides an analytical method for solving a typical class of differential equations of the form $\mathcal{H}(-i\frac{d}{dx})\Psi(x) = E\Psi(x)$ [86] in the large- L limit with homogeneous boundary conditions $\frac{d^k}{dx^k}\Psi(x=0) = 0$ and $\frac{d^l}{dx^l}\Psi(x=L) = 0$, where $\mathcal{H}(-id/dx)$ can be a matrix and its elements can have arbitrary order of $-id/dx$ and $k, l = 0, 1, 2, \dots$, which represent the order of the derivative with respect to x .

In summary, we predicted that the ultracold fermions with dissipative spin-orbit coupling have a robust NHSE. Since both the many-body interaction can be well controlled in

⁶In the SM [86] we use an exactly solvable model to demonstrate this point.

⁷It should be noted that our theory is consistent with the current experimental measurements of Ref. [36]. Although the momentum-resolved Rabi oscillation detected in Ref. [36] agrees with the free-particle spectrum, we cannot say the system does not have NHSE. The reason is that the NHSE cannot be detected by the short-time correlations far away from the boundary. In the Supplemental Material [86] we provide a detailed discussion and simulations to demonstrate this point.

⁸Experimentally, since the box potential has been realized in Refs. [90,91], we believe that the measurement of the distribution of fermion density over time which is often used in ultracold-atom technology [9,15,92] can be used to observe the DSE.

such a system, our proposal establishes an ideal platform to study the interplay between the NHSE and many-body interactions. We further showed that the NHSE is robust not only to external parameters but also to external trapping potentials. The latter can be understood from the perspective of a non-Hermitian bulk-boundary correspondence. Finally, we proposed a boundary effect related to the NHSE, that is, the DSE. This DSE not only provides a valuable method to identify the NHSE but also reveals that non-Hermitian systems with the NHSE violate the conventional reflection rule, which is an important physical consequence that deserves to be investigated in detail.

ACKNOWLEDGMENTS

This work was supported by the National Natural Science Foundation of China (Grant No. NSFC-11888101), and the Strategic Priority Research Program of Chinese Academy of Sciences (Grant No. XDB28000000). F.Z. and Z.Y. were supported in part by the Strategic Priority Research Program of Chinese Academy of Sciences Grant No. XDB28000000 and NSF China Grant No. 11674278. Z.Y. was also supported by the National Science Foundation of China (Grant No. NSFC-12104450), the fellowship of China National Postdoctoral Program for Innovative Talents (Grant No. BX2021300) and the fellowship of China Postdoctoral Science Foundation (Grant No. 2022M713108).

-
- [1] I. Bloch, *Nat. Phys.* **1**, 23 (2005).
 [2] D. Jaksch and P. Zoller, *Ann. Phys. (NY)* **315**, 52 (2005).
 [3] I. Bloch, J. Dalibard, and W. Zwerger, *Rev. Mod. Phys.* **80**, 885 (2008).
 [4] S. Giorgini, L. P. Pitaevskii, and S. Stringari, *Rev. Mod. Phys.* **80**, 1215 (2008).
 [5] D.-W. Zhang, Y.-Q. Zhu, Y. X. Zhao, H. Yan, and S.-L. Zhu, *Adv. Phys.* **67**, 253 (2019).
 [6] M. Atala, M. Aidelsburger, J. T. Barreiro, D. Abanin, T. Kitagawa, E. Demler, and I. Bloch, *Nat. Phys.* **9**, 795 (2013).
 [7] G. Jotzu, M. Messer, R. Desbuquois, M. Lebrat, T. Uehlinger, D. Greif, and T. Esslinger, *Nature (London)* **515**, 237 (2014).
 [8] N. Goldman, J. Dalibard, A. Dauphin, F. Gerbier, M. Lewenstein, P. Zoller, and I. B. Spielman, *Proc. Natl. Acad. Sci. USA* **110**, 6736 (2013).
 [9] J. F. Sherson, C. Weitenberg, M. Endres, M. Cheneau, I. Bloch, and S. Kuhr, *Nature (London)* **467**, 68 (2010).
 [10] M. E. Tai, A. Lukin, M. Rispoli, R. Schittko, T. Menke, B. Dan, P. M. Preiss, F. Grusdt, A. M. Kaufman, and M. Greiner, *Nature (London)* **546**, 519 (2017).
 [11] M. Aidelsburger, M. Atala, M. Lohse, J. T. Barreiro, B. Paredes, and I. Bloch, *Phys. Rev. Lett.* **111**, 185301 (2013).
 [12] M. Lohse, C. Schweizer, H. M. Price, O. Zilberberg, and I. Bloch, *Nature (London)* **553**, 55 (2018).
 [13] M. Lohse, C. Schweizer, O. Zilberberg, M. Aidelsburger, and I. Bloch, *Nat. Phys.* **12**, 350 (2016).
 [14] M. Mancini, G. Pagano, G. Cappellini, L. Livi, M. Rider, J. Catani, C. Sias, P. Zoller, M. Inguscio, M. Dalmonte, and L. Fallani, *Science* **349**, 1510 (2015).
 [15] S. Nakajima, T. Tomita, S. Taie, T. Ichinose, H. Ozawa, L. Wang, M. Troyer, and Y. Takahashi, *Nat. Phys.* **12**, 296 (2016).
 [16] W. Sun, B. Z. Wang, X. T. Xu, C. R. Yi, L. Zhang, Z. Wu, Y. Deng, X. J. Liu, S. Chen, and J. W. Pan, *Phys. Rev. Lett.* **121**, 150401 (2018).
 [17] Z. Wu, L. Zhang, W. Sun, X. T. Xu, B. Z. Wang, S. C. Ji, Y. Deng, S. Chen, X. J. Liu, and J. W. Pan, *Science* **354**, 83 (2016).
 [18] H. Kim, G. Zhu, J. V. Porto, and M. Hafezi, *Phys. Rev. Lett.* **121**, 133002 (2018).
 [19] L. Chen, P. Wang, Z. Meng, L. Huang, H. Cai, D. W. Wang, S. Y. Zhu, and J. Zhang, *Phys. Rev. Lett.* **120**, 193601 (2018).
 [20] T. Liu, Y. R. Zhang, Q. Ai, Z. Gong, K. Kawabata, M. Ueda, and F. Nori, *Phys. Rev. Lett.* **122**, 076801 (2019).
 [21] K. Sun, W. V. Liu, A. Hemmerich, and S. Das Sarma, *Nat. Phys.* **8**, 67 (2012).
 [22] X. Li, E. Zhao, and W. V. Liu, *Nat. Commun.* **4**, 1523 (2013).
 [23] B. Huang, Y. H. Wu, and W. V. Liu, *Phys. Rev. Lett.* **120**, 110603 (2018).
 [24] B. Huang and W. V. Liu, *Phys. Rev. Lett.* **124**, 216601 (2020).
 [25] R. A. Hart, P. M. Duarte, T. L. Yang, X. Liu, T. Paiva, E. Khatami, R. T. Scalettar, N. Trivedi, D. A. Huse, and R. G. Hulet, *Nature (London)* **519**, 211 (2015).
 [26] P. T. Brown, D. Mitra, E. Guardado-Sanchez, P. Schauß, S. S. Kondov, E. Khatami, T. Paiva, N. Trivedi, D. A. Huse, and W. S. Bakr, *Science* **357**, 1385 (2017).
 [27] A. Mazurenko, C. S. Chiu, G. Ji, M. F. Parsons, M. Kanasz-Nagy, R. Schmidt, F. Grusdt, E. Demler, D. Greif, and M. Greiner, *Nature (London)* **545**, 462 (2017).
 [28] D. Mitra, P. T. Brown, E. Guardado-Sanchez, S. S. Kondov, T. Devakul, D. A. Huse, P. Schauß, and W. S. Bakr, *Nat. Phys.* **14**, 173 (2018).
 [29] S. Diehl, A. Micheli, A. Kantian, B. Kraus, H. P. Büchler, and P. Zoller, *Nat. Phys.* **4**, 878 (2008).
 [30] V. A. Brazhnyi, V. V. Konotop, V. M. Perez-Garcia, and H. Ott, *Phys. Rev. Lett.* **102**, 144101 (2009).
 [31] S. Diehl, E. Rico, M. A. Baranov, and P. Zoller, *Nat. Phys.* **7**, 971 (2011).
 [32] D. A. Zezyulin, V. V. Konotop, G. Barontini, and H. Ott, *Phys. Rev. Lett.* **109**, 020405 (2012).
 [33] R. Labouvie, B. Santra, S. Heun, and H. Ott, *Phys. Rev. Lett.* **116**, 235302 (2016).
 [34] S. Lapp, J. Ang'ong'a, F. A. An, and B. Gadway, *New J. Phys.* **21**, 045006 (2019).
 [35] J. Li, A. K. Harter, J. Liu, L. de Melo, Y. N. Joglekar, and L. Luo, *Nat. Commun.* **10**, 855 (2019).
 [36] Z. Ren, D. Liu, E. T. Zhao, C. D. He, K. k. Pak, J. S. Li, and G. B. Jo, *Nat. Phys.* **18**, 385 (2022).
 [37] G. Barontini, R. Labouvie, F. Stubenrauch, A. Vogler, V. Guarrera, and H. Ott, *Phys. Rev. Lett.* **110**, 035302 (2013).
 [38] Y. Takasu, T. Yagami, Y. Ashida, R. Hamazaki, Y. Kuno, and Y. Takahashi, *Prog. Theor. Exp. Phys.* **2020**, 12A110 (2020).
 [39] D. Dast, D. Haag, H. Cartarius, and G. Wunner, *Phys. Rev. A* **90**, 052120 (2014).
 [40] L. Li, S. Mu, C. H. Lee, and J. Gong, *Nat. Commun.* **12**, 5294 (2021).

- [41] M. Nakagawa, N. Kawakami, and M. Ueda, *Phys. Rev. Lett.* **121**, 203001 (2018).
- [42] M. Nakagawa, N. Kawakami, and M. Ueda, *Phys. Rev. Lett.* **126**, 110404 (2021).
- [43] L. Pan, X. Chen, Y. Chen, and H. Zhai, *Nat. Phys.* **16**, 767 (2020).
- [44] K. Yamamoto, M. Nakagawa, K. Adachi, K. Takasan, M. Ueda, and N. Kawakami, *Phys. Rev. Lett.* **123**, 123601 (2019).
- [45] Y. Ashida, Z. Gong, and M. Ueda, *Adv. Phys.* **69**, 249 (2020).
- [46] Y. Xu, S. T. Wang, and L. M. Duan, *Phys. Rev. Lett.* **118**, 045701 (2017).
- [47] E. J. Bergholtz, J. C. Budich, and F. K. Kunst, *Rev. Mod. Phys.* **93**, 015005 (2021).
- [48] S. Lieu, M. McGinley, and N. R. Cooper, *Phys. Rev. Lett.* **124**, 040401 (2020).
- [49] S. Yao and Z. Wang, *Phys. Rev. Lett.* **121**, 086803 (2018).
- [50] S. Yao, F. Song, and Z. Wang, *Phys. Rev. Lett.* **121**, 136802 (2018).
- [51] F. Song, S. Yao, and Z. Wang, *Phys. Rev. Lett.* **123**, 246801 (2019).
- [52] F. K. Kunst, E. Edvardsson, J. C. Budich, and E. J. Bergholtz, *Phys. Rev. Lett.* **121**, 026808 (2018).
- [53] K. Yokomizo and S. Murakami, *Phys. Rev. Lett.* **123**, 066404 (2019).
- [54] K. Zhang, Z. Yang, and C. Fang, *Phys. Rev. Lett.* **125**, 126402 (2020).
- [55] N. Okuma, K. Kawabata, K. Shiozaki, and M. Sato, *Phys. Rev. Lett.* **124**, 086801 (2020).
- [56] Z. Yang, K. Zhang, C. Fang, and J. Hu, *Phys. Rev. Lett.* **125**, 226402 (2020).
- [57] V. M. Martinez Alvarez, J. E. Barrios Vargas, and L. E. F. Foa Torres, *Phys. Rev. B* **97**, 121401(R) (2018).
- [58] C. H. Lee and R. Thomale, *Phys. Rev. B* **99**, 201103(R) (2019).
- [59] F. Song, S. Yao, and Z. Wang, *Phys. Rev. Lett.* **123**, 170401 (2019).
- [60] C. H. Lee, L. Li, and J. Gong, *Phys. Rev. Lett.* **123**, 016805 (2019).
- [61] L. Li, C. H. Lee, and J. Gong, *Phys. Rev. Lett.* **124**, 250402 (2020).
- [62] D. S. Borgnia, A. J. Kruchkov, and R.-J. Slager, *Phys. Rev. Lett.* **124**, 056802 (2020).
- [63] S. Longhi, *Phys. Rev. Res.* **1**, 023013 (2019).
- [64] S. Longhi, *Phys. Rev. Lett.* **124**, 066602 (2020).
- [65] Y. Yi and Z. Yang, *Phys. Rev. Lett.* **125**, 186802 (2020).
- [66] L. Li, C. H. Lee, S. Mu, and J. Gong, *Nat. Commun.* **11**, 5491 (2020).
- [67] K. Zhang, Z. Yang, and C. Fang, *Nat. Commun.* **13**, 2496 (2022).
- [68] L. Xiao, T. Deng, K. Wang, G. Zhu, Z. Wang, W. Yi, and P. Xue, *Nat. Phys.* **16**, 761 (2020).
- [69] T. Helbig, T. Hofmann, S. Imhof, M. Abdelghany, T. Kiessling, L. W. Molenkamp, C. H. Lee, A. Szameit, M. Greiter, and R. Thomale, *Nat. Phys.* **16**, 747 (2020).
- [70] S. Weidemann, M. Kremer, T. Helbig, T. Hofmann, A. Stegmaier, M. Greiter, R. Thomale, and A. Szameit, *Science* **368**, 311 (2020).
- [71] T. Hofmann, T. Helbig, F. Schindler, N. Salgo, M. Brzezińska, M. Greiter, T. Kiessling, D. Wolf, A. Vollhardt, A. Kabašić, C. H. Lee, A. Bilušić, R. Thomale, and T. Neupert, *Phys. Rev. Res.* **2**, 023265 (2020).
- [72] T. Haga, M. Nakagawa, R. Hamazaki, and M. Ueda, *Phys. Rev. Lett.* **127**, 070402 (2021).
- [73] J. Claes and T. L. Hughes, *Phys. Rev. B* **103**, L140201 (2021).
- [74] X. Q. Sun, P. Zhu, and T. L. Hughes, *Phys. Rev. Lett.* **127**, 066401 (2021).
- [75] F. Schindler and A. Prem, *Phys. Rev. B* **104**, L161106 (2021).
- [76] P. M. Vecsei, M. M. Denner, T. Neupert, and F. Schindler, *Phys. Rev. B* **103**, L201114 (2021).
- [77] H. Hu and E. Zhao, *Phys. Rev. Lett.* **126**, 010401 (2021).
- [78] Z. Yang, [arXiv:2012.03333](https://arxiv.org/abs/2012.03333).
- [79] A. Ghatak, M. Brandenbourger, J. Wezel, and C. Coulais, *Proc. Natl. Acad. Sci. USA* **117**, 29561 (2020).
- [80] L. Xiao, T. Deng, K. Wang, Z. Wang, W. Yi, and P. Xue, *Phys. Rev. Lett.* **126**, 230402 (2021).
- [81] L. S. Palacios, S. Tchoumakov, M. Guix, I. Pagonabarraga, S. Sánchez, and A. G. Grushin, *Nat. Commun.* **12**, 4691 (2021).
- [82] X. Zhang, Y. Tian, J.-H. Jiang, M.-H. Lu, and Y.-F. Chen, *Nat. Commun.* **12**, 5377 (2021).
- [83] D. Zou, T. Chen, W. He, J. Bao, C. H. Lee, H. Sun, and X. Zhang, *Nat. Commun.* **12**, 7201 (2021).
- [84] L. Zhang, Y. Yang, Y. Ge, Y.-j. Guan, Q. Chen, Q. Yan, F. Chen, R. Xi, Y. Li, D. Jia, S.-q. Yuan, H.-x. Sun, H. Chen, and B. Zhang, *Nat. Commun.* **12**, 6297 (2021).
- [85] H. Zhai, *Int. J. Mod. Phys. B* **26**, 1230001 (2012).
- [86] See Supplemental Material at <http://link.aps.org/supplemental/10.1103/PhysRevA.106.L061302> for details, including generalized wave vectors theory, the robustness of skin effects, and further discussion of dynamic sticky effect, etc.
- [87] D. C. Brody, *J. Phys. A: Math. Theor.* **47**, 035305 (2014).
- [88] K. Kawabata, K. Shiozaki, M. Ueda, and M. Sato, *Phys. Rev. X* **9**, 041015 (2019).
- [89] Z. Gong, Y. Ashida, K. Kawabata, K. Takasan, S. Higashikawa, and M. Ueda, *Phys. Rev. X* **8**, 031079 (2018).
- [90] A. L. Gaunt, T. F. Schmidutz, I. Gotlibovych, R. P. Smith, and Z. Hadzibabic, *Phys. Rev. Lett.* **110**, 200406 (2013).
- [91] B. Mukherjee, Z. Yan, P. B. Patel, Z. Hadzibabic, T. Yefsah, J. Struck, and M. W. Zwierlein, *Phys. Rev. Lett.* **118**, 123401 (2017).
- [92] C. Weitenberg, M. Endres, J. F. Sherson, M. Cheneau, P. Schauss, T. Fukuhara, I. Bloch, and S. Kuhr, *Nature (London)* **471**, 319 (2011).